

Interplay between magnetic anisotropy and interlayer coupling in nanosecond magnetization reversal of spin-valve trilayers

J. Vogel,¹ W. Kuch,^{2,*} J. Camarero,³ K. Fukumoto,^{2,*} Y. Pennec,^{1,†} S. Pizzini,¹ M. Bonfim,⁴ F. Petroff,⁵ A. Fontaine,¹ and J. Kirschner²

¹Laboratoire Louis Néel, CNRS, 25 avenue des Martyrs, B.P. 166, 38042 Grenoble Cedex 9, France

²Max-Planck-Institut für Mikrostrukturphysik, Weinberg 2, 06120 Halle, Germany

³Dpto. Física de la Materia Condensada, Universidad Autónoma de Madrid, 28049 Madrid, Spain

⁴Departamento de Engenharia Elétrica, Universidade do Paraná, CEP 81531-990, Curitiba, Brazil

⁵Unité Mixte de Physique CNRS/Thales, Domaine de Corbeville, 91404 Orsay, France
and Université Paris-Sud, 91405 Orsay, France

(Received 26 May 2004; published 17 February 2005)

The influence of magnetic anisotropy on nanosecond magnetization reversal in coupled FeNi/Cu/Co trilayers was studied using a photoelectron emission microscope combined with x-ray magnetic circular dichroism. In quasi-isotropic samples the reversal of the soft FeNi layer is determined by domain-wall pinning that leads to the formation of small and irregular domains. In samples with uniaxial magnetic anisotropy, the domains are larger and the influence of local interlayer coupling dominates the domain structure and the reversal of the FeNi layer.

DOI: 10.1103/PhysRevB.71.060404

PACS number(s): 75.60.Jk, 75.60.Ch, 75.70.-i, 85.70.Kh

Magnetic trilayers in which two thin ferromagnetic films are separated by a nonmagnetic spacer layer present a variety of effects—giant magnetoresistance, tunnel magnetoresistance, spin torque transfer—that make them highly interesting for both fundamental studies and applications. Recent studies of magnetization dynamics of trilayer systems, such as spin valves (SV) and magnetic tunnel junctions (MTJ),^{1–5} are mainly motivated by magnetic recording and memory applications, since the switching speed of their active magnetic element, the soft ferromagnetic film, can ultimately limit the rate at which information can be read or written in the devices. At nanosecond time scales, the magnetization reversal of ferromagnetic layers is determined by processes such as nucleation and domain-wall propagation that are strongly sensitive to the magnetic anisotropy of the film. In magnetically coupled trilayers, also the interaction between the magnetic layers influences the reversal. Despite the fundamental interest of these effects and the consequences for technological applications, few studies have been published on the influence of interlayer coupling and anisotropy on the fast magnetization reversal of magnetically coupled trilayers.^{6–8} In this paper, we show that the magnetic anisotropy within the plane of the layers has a large influence on the shape of the magnetic domains and on the domain-wall dynamics, as well as on the correlation between the domain structures in the soft and hard magnetic layers. In quasi-isotropic samples the application of nanosecond magnetic pulses gives rise to small and irregular domains in the soft layer. This leads to a large density of 360° domain walls and consequently to a large increase of the saturation field. This phenomenon can be avoided using layers with a uniaxial magnetic anisotropy.

We have independently studied the nanosecond magnetization reversal of the soft permalloy (Fe₂₀Ni₈₀) and of the hard Co layer in spin-valve-like FeNi/Cu/Co trilayers using time- and layer-resolved photoelectron emission microscopy

(PEEM) combined with x-ray magnetic circular dichroism (XMCD).⁹ In XMCD-PEEM, secondary electrons emitted from the sample surface after resonant absorption of circularly polarized x rays are collected in an electron microscope to obtain an image of the magnetic domain structure. The magnetic contrast is caused by the difference in x-ray absorption of magnetic domains having their magnetization parallel or antiparallel to the direction of the incoming circularly polarized x rays. X-ray imaging techniques have been used to investigate magnetization dynamics mainly in Permalloy structures,^{10,11} but the chemical selectivity that can provide layer-resolved imaging has been little exploited.^{12,13}

The measurements were performed at the UE52-SGM and the UE56/2-PGM2 helical undulator beamlines of the BESSY synchrotron-radiation source in Berlin, Germany. Temporal resolution was obtained using a pump-probe scheme, like in our previous time-resolved XMCD measurements.² Magnetic pulses provided by a microcoil were synchronized with the photon bunches at a repetition rate of 625 kHz and images were acquired with different delays between the magnetic and photon pulses. The acquisition time per image was 5–10 mins, corresponding to an average over several hundreds of millions of pulses. More details can be found in Ref. 10. The setup of the electrostatic photoelectron emission microscope (Focus IS-PEEM) was described in Ref. 14. The angle of incidence of x rays on the sample was 60° from the surface normal. The photon energy was tuned to the Fe-L₃ (Co L₃) absorption edge to image the Permalloy (Co) domain structure. The electrons emitted by the Co layer had to travel through 12 nm of other material to reach the surface, leading to a weaker contrast for the Co images.

Two different Fe₂₀Ni₈₀/Cu/Co trilayers deposited on SiO₂/Si(001) substrates by rf sputtering were studied. The thickness of the Permalloy and Cu layers, 5 and 4 nm, respectively, was the same for both samples. The Co thickness

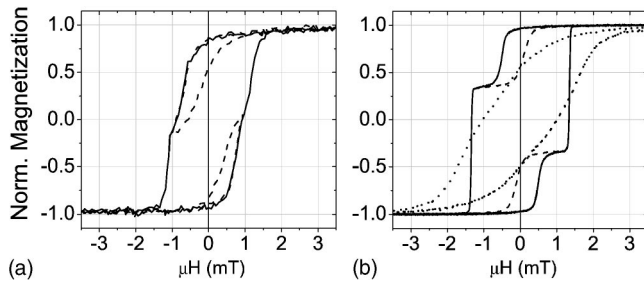


FIG. 1. Major and minor hysteresis loops obtained by longitudinal Kerr effect for two $\text{Fe}_{20}\text{Ni}_{80}(5 \text{ nm})/\text{Cu}(4 \text{ nm})/\text{Co}(x \text{ nm})$ spin-valve-like trilayers deposited on $\text{Si}(001)/\text{SiO}_2$. Sample A ($x=5$) is quasi-isotropic within the plane of the layers while sample B ($x=8$) presents uniaxial magnetic anisotropy. Minor loops of the FeNi layer are indicated by dashed lines. For sample B, both the in-plane easy (continuous line) and hard (dotted line) magnetization axis loops are shown.

was 5 nm for sample A and 8 nm for sample B. The samples were capped with an Al layer of 3 nm to protect them from oxidation. Quasistatic hysteresis loops obtained using longitudinal magneto-optical Kerr effect are shown in Fig. 1. The magnetization of both samples was in the plane of the layers. Hysteresis loops taken with the magnetic field applied along several azimuthal angles revealed no clear magnetic anisotropy within this plane for sample A. A small in-plane magnetic field applied during the growth of sample B led to a uniaxial magnetic anisotropy for the Permalloy layer, with the easy axis parallel to the applied field direction. Both samples show two transitions at different fields, corresponding to the separate reversal of the Permalloy (lower coercivity) and Co layers. The minor loops of the Permalloy layer (indicated by dashed lines in Fig. 1) are shifted with respect to zero field due to a coupling with the Co layer of about 0.4 mT in both samples. This magnetostatic coupling is due to correlated roughness at the two ferromagnetic/nonmagnetic interfaces.¹⁵ The hysteresis loops are more tilted for sample A. As we will see later, this indicates a lower barrier for nucleation than for sample B and a larger influence of the pinning of domain-wall motion.

For the time-resolved XMCD-PEEM imaging, we first induced a magnetic domain structure in the Co layer before investigating the Permalloy magnetization reversal. This allows to study, in a same image series, the behavior of the Permalloy layer for reversal against and with the local coupling direction, as well as the effect of the Co domain walls. For the image series of sample A in Fig. 2, the magnetization of the sample was first saturated in the negative direction. Then bipolar magnetic pulses were applied with the temporal shape shown in Fig. 2(a) and maximum and minimum field strengths of 5.4 and -2 mT. The repeated application of these pulses led after a short time to the zero-field domain structures shown in Fig. 2(b) for Permalloy and in Fig. 2(f) for Co. After these first few pulses, the Co domain structure remained stable.¹² Images were then acquired for different delays and representative images of the FeNi domain structure, taken for the delays indicated in Fig. 2(a), are shown in Figs. 2(b)–2(e). The Co domain image in Fig. 2(f) was recorded for a delay of -15 ns, but the domain structure was

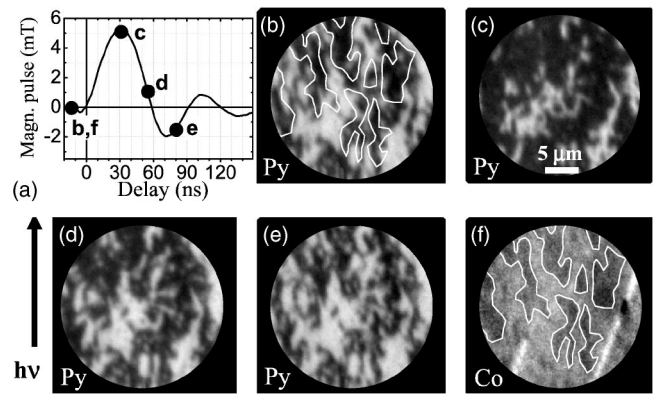


FIG. 2. Time- and layer-resolved XMCD-PEEM domain images of the Permalloy [(b)–(e)] and Co layers (f) of sample A. The field of view is about $25 \mu\text{m}$ and the spatial resolution $0.3 \mu\text{m}$. The projection of the x-ray incidence direction on the sample surface is pointing up in the images (parallel to the arrow) and is parallel (antiparallel) to the direction of the field for positive (negative) pulses. The magnetization direction is in the plane of the layers and points up (parallel to the arrow) for black domains, and down for white domains. The images were taken for delays between photon and magnetic pulses of -15 , 30, 55, and 80 ns, as indicated in (a). The clearest visible black domains in the Co layer are indicated with thin white lines in (f) and in the Permalloy image of (b) for comparison.

the same for other delays. The magnetic contrast in these time-resolved images was identical to the one of static images, indicating reproducible reversal for this sample. The reversal of the Permalloy layer magnetization takes place mainly through propagation of existing domain walls. The positive part of the magnetic-field pulses favors the growth of black domains [Fig. 2(c)], while negative fields favor the growth of white domains [Fig. 2(e)]. In Fig. 2(d) the size of the white domains increases compared to Fig. 2(c), while the field is still in the positive direction. In order to explain this the local coupling between the Permalloy and cobalt layers across the Cu spacer layer has to be taken into account.

The largest and clearest black domains in the Co layer are highlighted by thin white lines in Fig. 2(f). These lines are transposed to the Permalloy image in Fig. 2(b), at zero applied field, for comparison. Clearly some correlation between the two domain patterns exists, due to the magnetostatic coupling between the layers. However, this coupling is not sufficient to induce a parallel alignment between the local magnetization directions everywhere in the two magnetic layers, and other parameters play a role in determining the exact domain pattern of the Permalloy layer. In Fig. 2(e), for example, some black domains persist in the Permalloy layer above white domains in the Co layer, even if in that case both the external field and the local coupling with the Co favor white domains. Some white domains are also pinned on large defects that are clearly visible in the Co image. These results will be discussed in more detail below.

Time-resolved XMCD-PEEM images for sample B are shown in Fig. 3. A domain pattern [Fig. 3(f)] was first created in the Co layer using 1-ms-long pulses from an external coil. Bipolar magnetic pulses with the temporal shape shown

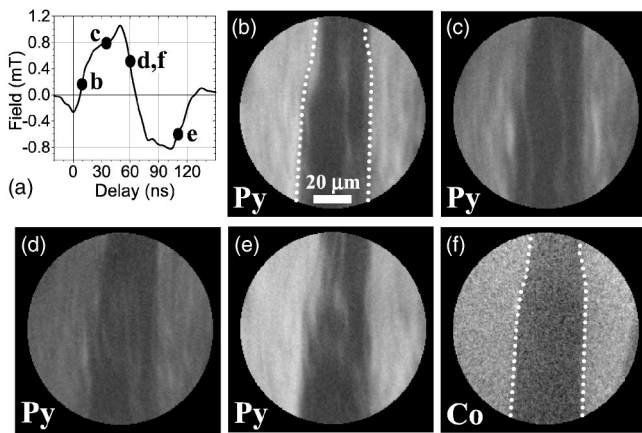


FIG. 3. Time- and layer-resolved XMCD-PEEM domain images of the Permalloy [(b)–(e)] and Co (f) layers of sample *B*. The field of view is about $80\ \mu\text{m}$ and the spatial resolution $1\ \mu\text{m}$. The direction of incoming photons and the magnetization directions of the different domains are the same as in Fig. 2. The images were taken at delays of 10, 35, 60, and 110 ns between photon and magnetic pulses, as indicated in (a). The dotted white lines in (b) and (f) indicate the position of the domain walls in the Co layer.

in Fig. 3(a) were then applied, with maximum and minimum field strengths of about 1 and $-0.8\ \text{mT}$. The amplitude of these pulses was too small to affect the Co domain pattern. At the beginning of the pulse, for an applied field close to zero [Fig. 3(b)], the correlation between the Permalloy and Co domain structures is much larger than in sample *A*. When the field increases, regions in the Permalloy that are white before the pulse become almost homogeneously gray instead of showing a domain structure [Figs. 3(c) and 3(d)]. This is caused by a nonreproducibility of the Permalloy domain structure, as demonstrated by static images of the FeNi layer acquired after the application of single magnetic pulses (Fig. 4). In this case, the Co layer presented a black domain on the left and a white domain on the right, separated by a domain wall as indicated on the Permalloy images with a thin white line. Images were obtained after application of 1, 9, and 14 pulses [for Figs. 4(a)–4(c), respectively] with shape and amplitude as in Fig. 3(a). The domains are smaller than those obtained after application of quasistatic pulses, but much larger than the domains in sample *A*. The domain walls travel over relatively large distances (tens of microns) upon reversal, and the domain structure is much less reproducible than

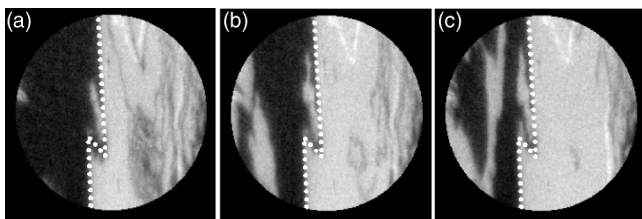


FIG. 4. Static XMCD-PEEM domain images of the Permalloy layer of sample *B*, taken after the application of 1, 9, and 14 pulses as shown in Fig. 3(a). Two domains are present in the Co layer, a black domain on the left and a white domain on the right, separated by a domain wall indicated in the images by a dotted white line.

in sample *A*. In pump-probe mode, the obtained images are an average over all different domain configurations, explaining the gray contrast observed for the Permalloy layer in Fig. 3.

A comparison between the different results shows that the domain patterns, the reproducibility of the switching, and the correlation between Permalloy and Co domain structures, are very different for both samples. Image series recorded with different pulsed field amplitudes and starting from different domain patterns in the Co layer did not show qualitative differences in the magnetization reversal of the Permalloy layer with respect to the representative series shown here. Since both samples were deposited on the same substrates using the same technique, and their quasistatic coercivity and interlayer coupling strength are quite similar, we attribute these differences in dynamic behavior to the difference in magnetic anisotropy.

In sample *A* the domains are some microns small and irregular. For magnetic media with perpendicular anisotropy, the regularity of the domain shape is determined by the domain-wall stiffness,^{16–18} which increases with increasing anisotropy. In sample *A*, the weak magnetic anisotropy within the plane leads to a relatively small domain-wall stiffness. Domain walls are easily distorted by pinning centers, leading to the irregular domain shapes observed in Fig. 2 and to the formation of a large number of 360° domain walls.¹² The application of short, strong, magnetic-field pulses increases this tendency by increasing the nucleation density.⁵ As a result, the magnetization is hard to saturate after application of short pulses, even using quasistatic pulses. The local coupling with the Co layer across the Cu spacer influences the local magnetization reversal of the Permalloy layer, but due to the large deformability of the domain walls the detailed domain pattern is determined mainly by local pinning. The geometry of the domains and the distance between them also plays a role in the reversal, as we showed in another paper.¹³

The domains in sample *B* are much larger than in sample *A*. The domain walls are essentially straight and parallel to the easy axis. Domain walls parallel to the magnetization direction accumulate less magnetic charges and are therefore less energetic than domain walls in other directions. The larger domain-wall stiffness than in sample *A*, due to the magnetic anisotropy, apparently causes pinning centers to play a less important role in determining the domain shape during magnetization reversal, which is dominated by magnetostatic effects like the local coupling with the Co layer.

The domain pattern observed during reversal is much less reproducible in sample *B* than in sample *A*. In general, domain walls propagate by Barkhausen jumps, from a couple of pinning centers to the next. These jumps can be quite reproducible when domain walls move back and forth over small distances,¹⁹ as in sample *A*. In sample *B*, the more rigid domain walls can be blocked by pinning centers, until the accumulated Zeeman energy is large enough to overcome the pinning barrier. By then, the domain wall will have acquired enough energy to overcome a great number of pinning centers, giving rise to Barkhausen “avalanches” that are less reproducible.

We can now also explain why much stronger pulses had to be used in sample *A* (Fig. 2) than in sample *B* (Fig. 3),

while the quasistatic coercivities are very similar. In the hysteresis loops the Permalloy layer is initially saturated and domains have to nucleate before the magnetization can reverse. When domains are already present, like in the time-resolved PEEM measurements, the relevant magnetic field is the one needed to cause domain-wall propagation and this field is smaller for sample *B* than for sample *A*. Moreover, coercivity and saturation fields strongly increase upon increasing the applied field sweep rate.^{5,20} We have performed Kerr loop measurements for different field sweep rates indicating that the increase of the saturation field going from quasistatic measurements to nanosecond field pulses is much larger for sample *A* than for sample *B*. We attribute this faster increase to the larger domain-wall pinning and the formation of many 360° domain walls.

In summary, we have used XMCD-PEEM to study magnetization reversal in spin-valve-like trilayers with spatial, temporal, and layer resolution. We show that magnetic anisotropy has an important influence on the soft layer magnetization reversal. In the presence of a uniaxial magnetic anisotropy within the plane the correlation between the domain

structures in the soft and hard magnetic layers is strong. When this anisotropy is absent or very small, local pinning effects mainly determine the domain structure upon reversal.

These results also illustrate why in applications using fast magnetization switching the presence of magnetic anisotropy within the plane of the layers should be preferred. For a soft magnetic layer without such a magnetic anisotropy, the application of short magnetic pulses induces the formation of small domains and of many 360° domain walls. This leads to a large increase of the field needed to magnetically saturate the sample.

We thank A. Vaurès and Y. Conraux for sample preparation. Financial support by BMBF (No. 05, KS1EFA6), EU (BESSY-EC-HPRI Contract No. HPRI-1999-CT-00028), and the Laboratoire Européen Associé “Mesomag” is gratefully acknowledged. J.C. acknowledges support through a “Ramón y Cajal” contract and through Project No. MAT2003-08627-C02-02 from the Spanish Ministry of Science and Technology.

*Present address: Institut für Experimentalphysik, Freie Universität Berlin, Arnimallee 14, 14195 Berlin, Germany.

†Present address: Department of Physics, University of Alberta, Edmonton, Alberta, Canada T6G 2J1.

¹H. W. Schumacher, C. Chappert, P. Crozat, R. C. Sousa, P. P. Freitas, J. Miltat, J. Fassbender, and B. Hillebrands, *Phys. Rev. Lett.* **90**, 017201 (2003).

²M. Bonfim, G. Ghiringhelli, F. Montaigne, S. Pizzini, N. B. Brookes, F. Petroff, J. Vogel, J. Camarero, and A. Fontaine, *Phys. Rev. Lett.* **86**, 3646 (2001).

³S. Kaka and S. E. Russel, *Appl. Phys. Lett.* **80**, 2958 (2002).

⁴B. Heinrich, Y. Tserkovnyak, G. Woltersdorf, A. Brataas, R. Urban, and G. E. W. Bauer, *Phys. Rev. Lett.* **90**, 187601 (2003).

⁵Y. Pennec, J. Camarero, J. C. Toussaint, S. Pizzini, M. Bonfim, F. Petroff, W. Kuch, F. Offi, K. Fukumoto, F. Nguyen Van Dau, and J. Vogel, *Phys. Rev. B* **69**, 180402(R) (2004).

⁶J. Fassbender and M. Bauer, *Europhys. Lett.* **55**, 119 (2001).

⁷R. J. Hicken, A. Barman, V. V. Kruglyak, and S. Ladak, *J. Phys. D* **36**, 2183 (2003).

⁸A. Layadi, *J. Magn. Magn. Mater.* **266**, 282 (2003).

⁹C. M. Schneider and G. Schönhense, *Rep. Prog. Phys.* **65**, R1785 (2002).

¹⁰J. Vogel, W. Kuch, M. Bonfim, J. Camarero, Y. Pennec, F. Offi, K. Fukumoto, J. Kirschner, A. Fontaine, and S. Pizzini, *Appl. Phys. Lett.* **82**, 2299 (2003).

¹¹C. M. Schneider, A. Kuksov, A. Krasnyuk, A. Oelsner, D. Neeb, S.

A. Nepijenko, G. Schönhense, I. Mönch, R. Kaltofen, J. Morais, C. De Nadaï, and N. B. Brookes, *Appl. Phys. Lett.* **85**, 2562 (2004); H. Stoll, A. Puzic, B. van Waeyenberge, P. Fischer, J. Raabe, M. Buess, T. Haug, R. Höllinger, C. Back, D. Weiss, and G. Denbeaux, *ibid.* **84**, 3328 (2004); S. B. Choe, Y. Acremann, A. Scholl, A. Bauer, A. Doran, J. Stöhr, and H. A. Padmore, *Science* **304**, 420 (2004).

¹²J. Vogel, W. Kuch, J. Camarero, K. Fukumoto, Y. Pennec, M. Bonfim, S. Pizzini, F. Petroff, A. Fontaine, and J. Kirschner, *J. Appl. Phys.* **95**, 6533 (2004).

¹³W. Kuch, J. Vogel, J. Camarero, K. Fukumoto, Y. Pennec, S. Pizzini, M. Bonfim, and J. Kirschner, *Appl. Phys. Lett.* **85**, 440 (2004).

¹⁴W. Kuch, R. Frömter, J. Gilles, D. Hartmann, Ch. Ziethen, C. M. Schneider, G. Schönhense, W. Swiech, and J. Kirschner, *Surf. Rev. Lett.* **5**, 1241 (1998).

¹⁵L. Néel, *C. R. Hebd. Seances Acad. Sci.* **255**, 1676 (1962).

¹⁶A. A. Thiele, *Bell Syst. Tech. J.* **48**, 3287 (1969).

¹⁷H. P. D. Shieh and M. H. Kryder, *J. Appl. Phys.* **61**, 1108 (1987).

¹⁸M. Kisielewski, A. Maziewski, M. Tekielak, J. Ferré, S. Lemerle, V. Mathet, and C. Chappert, *J. Magn. Magn. Mater.* **260**, 231 (2003).

¹⁹J. S. Urbach, R. C. Madison, and J. T. Markert, *Phys. Rev. Lett.* **75**, 4694 (1995).

²⁰E. M. Gyorgy, *J. Appl. Phys.* **28**, 1011 (1957).